ADAPTIVE COMPOSITE RUBBER BEARINGS FOR TIMBER STRUCTURE: A CASE STUDY FOR EARTHQUAKE-PRONE REGIONS

W.C. Liao[1], Kin Sang Michael Wong[2]

ABSTRACT: Mass timber buildings are becoming more popular in Europe and America for its low carbon footprint compared with traditional construction materials. However, its earthquake resistance should be carefully considered if it is to be used in earthquake-prone areas such as the Asia-Pacific region. The use of traditional base isolators such as lead rubber bearing was already prohibited in Europe due to its toxic gas emission during melting of lead core when large displacement occurs. Therefore, alternative bearing such as adaptive composite rubber bearing (ACRB) made with more environmental-friendly material is being developed. This study applies carbon fabric, layered rubber sheet and novel core materials to fabricate an ACRB base isolator with adjustable damping ratio and lateral shear stiffness. A quasi-isotropic layup of carbon fabric, high temperature resin prepreg system and hot press is adopted in the fabrication of composite laminates. The selection of primer coat between composites and raw rubber is determined by the double lap shear test of a single composite/rubber unit. Through the biaxial test of this novel ACRB base isolator, the equivalent damping ratio, equivalent lateral stiffness and friction coefficient of the isolator can be characterized. Under low shear strain, the damping ratio of the isolator can be as high as 0.58, and the envelopes of their hysteretic loop shows prominent seismic energy absorption capacity. In order to verify the earthquake mitigation performance of these adaptive composite rubber bearings, shaking table tests of several down-scaled multi-story mass timber buildings were carried out.

KEYWORDS: Mass timber building, adaptive rubber bearing, carbon fabric, biaxial test, shaking table seismic test

1 INTRODUCTION

Mass timber buildings includes cross laminated timber (CLT), glued laminated timber (GLT) and dowel laminated timber (DLT) are popular construction materials used for medium to tall buildings in Europe and America. The reason for the trend to use more timber over conventional construction materials is due to its low carbon footprint and urban heat island effect. With the improvement of timber material against fire, corrosion and pest, it is foreseen that timber would become more popular in other urban areas. In order to improve the earthquake resistance of timber buildings, the most cost-effective way would be by the implementation of passive control measures at the base of the timber structure.

During an earthquake, energy was transferred into buildings through forced vibration. As the major frequency of earthquake shown in typical response spectrum coincides with the natural frequency (1-10Hz) of conventional building structures, resonance effect would be resulted during an earthquake. The structural members would exhibit large internal force during resonance vibration and be damaged. Passive isolation makes use of the low stiffness of the isolator to change the natural frequency of the above building to lower than 0.5Hz. Passive control measures include three major principles: base isolation, energy dissipation and vibration mitigation. Energy dissipation method relies on the hysteretic damping through yielding of metal core, friction damping or viscous damping to provide supplementary damping to dissipate the vibration response of the structure.

This study aimed at fabricating an adaptive composite elastomeric base isolator and verify its performance in mass timber structure. In the past, high damping rubber bearing (HDRB) and lead rubber bearing (LRB) were efficient elastomeric base isolators to make use of the low strength of rubber to change the frequency of the structure and dissipate the earthquake energy transferred up to the structure. The addition of lead core could even provide larger energy dissipation through the plastic deformation of the core during extremely large displacement [2][3]. However, in 2009, Kalpakidis and Constantinou [4][5] carried out studies on the effects of heating on the behaviour of lead-core rubber bearings and concluded that the lead core would have zero yield strength when it reached its melting point at 327ºC and thus the earthquake energy would be absorbed by the adjacent rubber and resulted in its damage and failure. During the Tohoku earthquake in Japan in 2011, some of the lead core in LRB were found to be having irreversible deformation due to the sudden rise in temperature resulted from extremely large displacement[6][7]. The European Union had banned the use of lead core in LRB in 2011. Therefore, it is urgent to find alternative laminate material that could replace the function of lead core in rubber bearing.

[1] W.C. Liao, Department of Civil Engineering, Feng Chia University, Taiwan, wcliao@fcu.edu.tw

[2] Kin Sang Michael Wong, Department of Civil Engineering, Feng Chia University, Taiwan, m1083495@o365.fcu.edu.tw

In contrary to LRBs, HDRB uses laminated specialized high damping rubber (HDR) and had slightly lower energy dissipation capacity [8].

In this study, carbon fabric, layered rubber sheet and novel core materials were used to fabricate an ACRB base isolator with adjustable damping ratio and lateral shear stiffness. A quasi-isotropic layup of carbon fabric, high temperature prepreg resin system and hot press is adopted in the fabrication of composite laminates. The selection of primer coat between composites and raw rubber is determined by the double lap shear test of a single composite/rubber unit. Through the biaxial test of this novel ACRB base isolator, the equivalent damping ratio, equivalent lateral stiffness and friction coefficient of the isolator can be characterized. Under low shear strain, the damping ratio of the isolator can be as high as 0.58, and the envelopes of their hysteretic loop shows prominent seismic energy absorption capacity. In order to verify the earthquake mitigation performance of these adaptive composite rubber bearings, shaking table tests of several down-scaled multi-story mass timber buildings were carried out.

2 CHARACTERISTICS TEST OF ACRB

2.1 DESIGN AND MANUFACTURING OF AN ADAPTIVE FIBER-REINFORCED RUBBER BEARING BASE ISOLATOR

Carbon roving TC360 from Formosa Plastic Group has a tensile modulus of 250 GPa, and tensile strength of 4890 MPa, respectively, were adopted in this research. The UD carbon laminate has E_1=117.29 GPa, E_2=E_3=7.44 GPa, G_{12}=3.77GPa, and v_{12} = 0.1946. In order to avoid the misalignment in the curing of composite laminate and rubber layers, a quasi-isotropic stacking sequence of [0/90/+45/-45]s is adopted. All carbon plates were made through hot press to about 3mm thick. High temperature resin prepreg of EPO-HTG™ G351N from Epotech Taiwan was applied during the layup. The carbon plates were then cut to Φ130mm discs and stacked with Φ60mm shim core steel plates and sliding plates to form the core of the ACRB. The outer side of the core layer were filled up by high damping rubber. From 3-D effective moduli theory, we can estimate E_x=E_y = 44.66 GPa, which are close to experimental data. The layup of an adaptive composite rubber bearing is shown in Figure 1.

2.2 BIAXIAL TEST ON ACRB

Biaxial test was used to test the ACRB under different frequency, loading directions and shear strain. The typical experimental setup for ACRB is shown in Figure 2. After setting a vertical force, horizontal displacement would applied through the MTS dynamic system with sine wave movement at different frequencies and amplitudes. Vertical force, horizontal force and displacement were recorded by imc μ-sys to yield hysteresis loops.
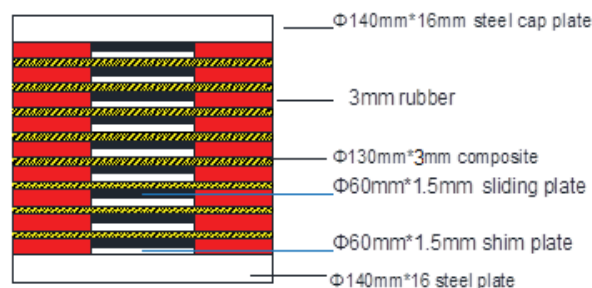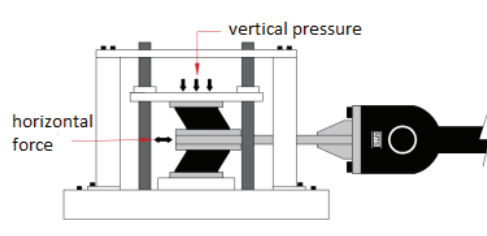

Figure 1: Scaled down ACRB

Figure 2: Setup for biaxial test

2.3 SHAKING TABLE TEST FOR SCALED TIMBER STRUCTURE WITH ACRB

Four scaled ACRB were then installed under a scaled 3-storey steel structure which was designed to have the weight and natural frequency similar to timber structure to carry out the shaking table test. The earthquake loading used were scaled-down El Centro earthquake (1940) and Chi-Chi earthquake (1999) under x and y directions separately. Control tests with no ACRB were also recorded for comparison with the use of scaled-down earthquakes at 0.05g to prevent extensive damage to the structure. Accelerometers and displacement gauges were installed at every storey to record the acceleration and displacement in x and y directions as shown in Figure 3 and 4. The reason for the use of steel structure instead of real timber structure was due to the consideration on transportation and size limit of the shaking table.

3 RESULTS AND DISCUSSION

3.1 BIAXIAL TEST ON ACRB

Biaxial tests were carried out under 5t(3.7MPa) & 7t(5.2MPa) vertical force with sine wave signals at different frequencies (0.1Hz, 0.2Hz, 0.5Hz, 1.0Hz & 1.5Hz) and different horizontal shear strain (25%, 50%, 100% & 150%) of the total thickness of rubber. Typical hysteresis loops for two repeated cycles under different shear strains are shown in Figure 5 and Figure 6.

The data obtained from the hysteresis loops was used to calculate the effective stiffness (K_{eff}) as demonstrated by Liao, Tsai and Hsieh [9] by the following Equation (1):
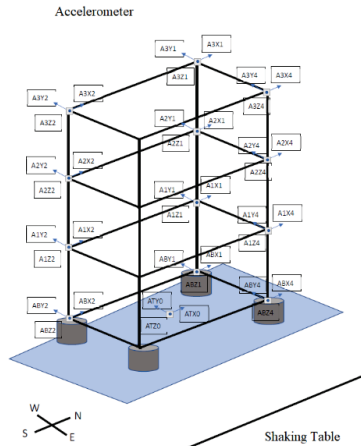
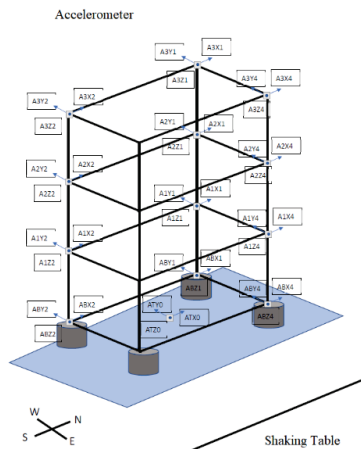Figure 3: Setup for accelerometers for shaking table test

Figure 4: Setup for displacement gauges for shaking table test

$$K_{eff} = \frac{F_i^+ - F_i^-}{2\Delta_i} \quad (1)$$

where F_i^+ = maximum horizontal force of ith cycle,
         F_i^- = minimum horizontal force of ith cycle,
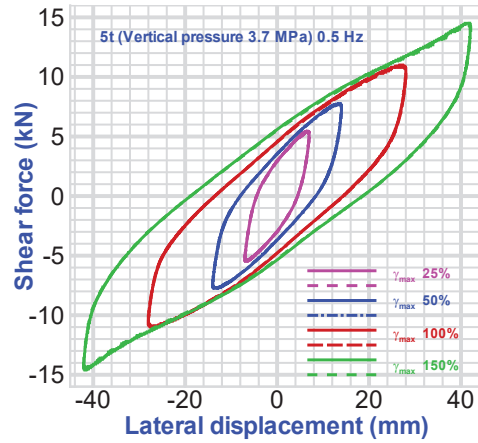 Δ_i = average horizontal displacement of ith cycle.

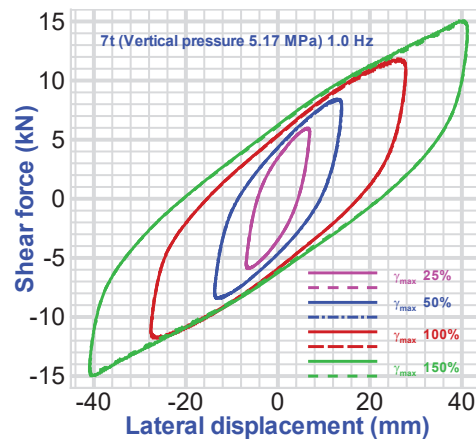Figure 5: Hysteresis loop of ACRB at different shear strains under pressure of 3.7MPa at 0.5Hz frequency

Figure 6: Hysteresis loop of ACRB at different shear strains under pressure of 5.2MPa at 1.0Hz frequency

The effective stiffness (K_{eff}) was plotted against the shear strain under different frequencies of loading. As shown in Figure 7 and 8 below, K_{eff} decreased significantly when the shear strain increased. The effect on frequencies was relatively insignificant.
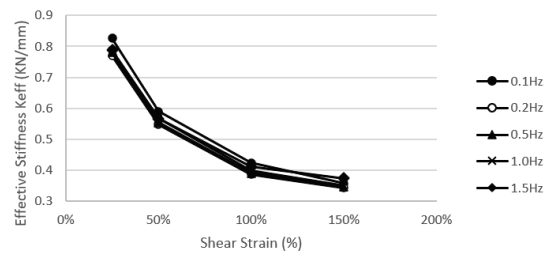

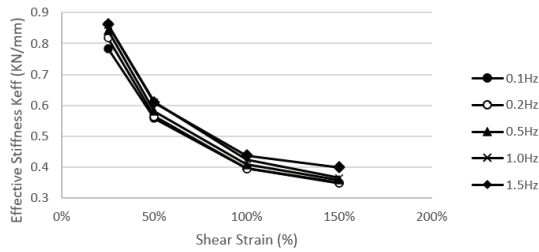Figure 7: Effective stiffness against shear strain under pressure of 3.7MPa

Figure 8: Effective stiffness against shear strain under pressure of 5.2MPa

The equivalent damping ratio (ξ_e^i) as demonstrated by Liao, Tsai and Hsieh [9] by the following Equation (2):

$$\xi_e^i = \frac{E_d^i}{2\pi \, k_{eff}^i \Delta_i^2} \qquad (2)$$

where E_d^i= area enclosed by ith cycle in loop.

The test results of equivalent damping ratio under 5t (3.7MPa) and 7t (5.2MPa) are summarized in Table 1 and Table 2 below:

Table 1: Equivalent damping ratio ξ_e^i of ACRB under 5t(3.7MPa) vertical pressure.

Shear strain	Frequency				
	0.1Hz	0.2Hz	0.5Hz	1.0Hz	1.5Hz
25%	24.7%	27.5%	27.6%	28.0%	28.3%
50%	22.5%	24.9%	25.2%	25.6%	26.0%
100%	19.8%	22.7%	23.1%	23.4%	23.4%
150%	18.0%	19.1%	19.5%	20.2%	22.2%

Table 2: Equivalent damping ratio ξ_e^i of ACRB under 7t(5.2MPa) vertical pressure.

Shear strain	Frequency				
	0.1Hz	0.2Hz	0.5Hz	1.0Hz	1.5Hz
25%	27.9%	28.5%	28.4%	29.4%	29.7%
50%	27.0%	27.6%	27.8%	28.2%	28.7%
100%	24.3%	24.7%	25.5%	26.1%	26.1%
150%	21.4%	21.4%	22.3%	22.4%	25.5%

As shown in the tables above, the equivalent damping ratio is relatively insensitive to frequency of loading. However, it increased when the vertical pressure increased and dropped when the shear strain increased.

3.2 SHAKING TABLE TEST FOR SCALED TIMBER STRUCTURE WITH ACRB

From the shaking table results, the inter-storey displacement and relative acceleration were both significantly reduced after ACRB were installed. The displacement of each storey in x-direction under 0.5g El Centro (NS) earthquake was plotted against time in Figure 9 below:
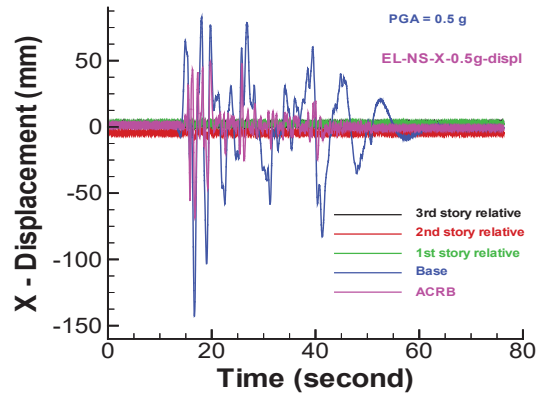

Figure 9: Displacement of base and relative displacement of different storeys under PGA of 0.5g El Centro (NS) Earthquake.

The above figure showed that the relative displacement of the structure itself was small and not more than 5mm. When compared with the base displacement (with maximum at about 140mm), the inter-storey movement was almost negligible and the structure was shaking with rigid body motion.

A typical plot about the acceleration at different storeys against time is shown in Figure 10 below.
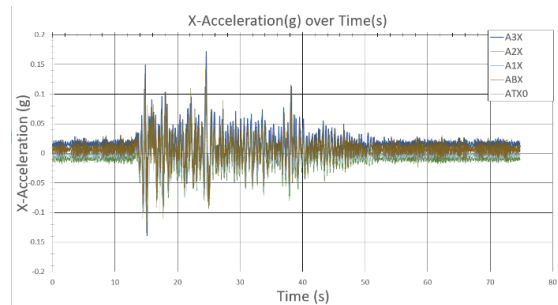

Figure 10: Acceleration of base, ACRB and each storey under PGA of 0.2g El Centro Earthquake.

The peak acceleration of each storey within the earthquake was extracted for comparison to calculate the acceleration reduction efficiency of the ACRB. The ratio for comparison would be by comparing the peak ground acceleration (PGA) actually measured by 0.05g loading of the same earthquake. The summary on acceleration reduction efficiency of El Centro-NS loading were compared in Table 3 below.

Table 3: Acceleration reduction efficiency of ACRB under different levels of El Centro (NS) loading

	w/o ACRB	w/ ACRB		
Test name	0.05g	0.2g	0.3g	0.4g
PGA (g)	0.060	0.181	0.320	0.424

3F	0.099	0.170	43%	0.371	29%	0.397	43%
2F	0.082	0.154	37%	0.222	49%	0.311	46%
1F	0.068	0.157	23%	0.317	12%	0.358	25%

In order to further check the damping efficiency of the ACRB under earthquake loadings, the base shear was plotted against the average x-displacement of the ACRB to show the relationship between ACRB displacement and base shear under various earthquake acceleration. The base shear was calculated based on the sum of the products of storey mass times average acceleration in x direction for each storey. The result of the hysteresis loops were shown in Figure 11-16 below.

As shown in Figure 11, 14 & 15 where the shear strain was up to 138%, the equivalent damping ratio was up to 23.7%. As shown in Figure 13, 14 & 16 where the shear strain was up to 256%, the equivalent damping ratio would gradually decrease to 15.8%.
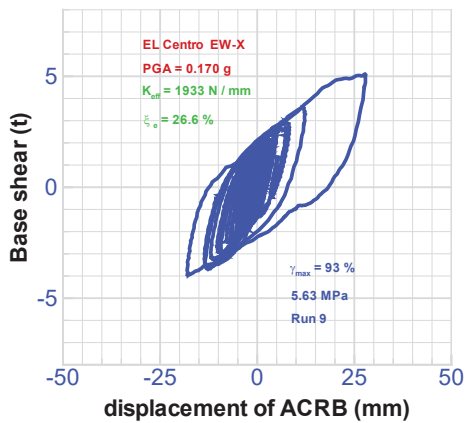

Figure 13: Hysteresis loop of ACRB under PGA of 0.318g Chi-Chi NS Earthquake...

Figure 11: Hysteresis loop of ACRB under PGA of 0.170g El Centro EW Earthquake.

Figure 14: Hysteresis loop of ACRB under PGA of 0.207g El Centro EW Earthquake.
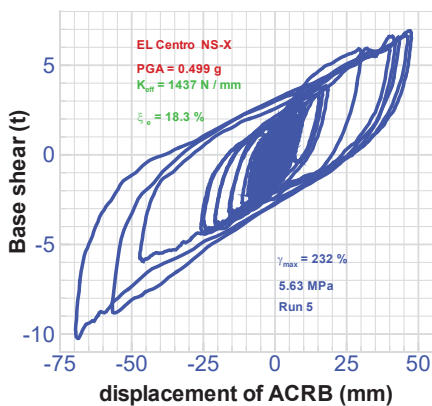

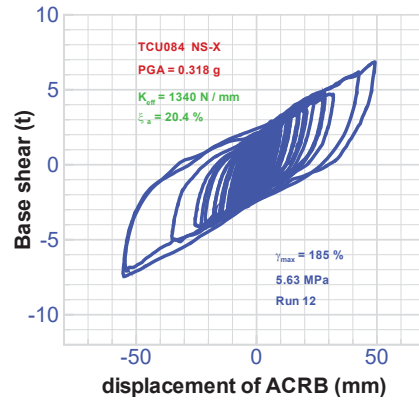Figure 12: Hysteresis loop of ACRB under PGA of 0.499g El Centro NS Earthquake.

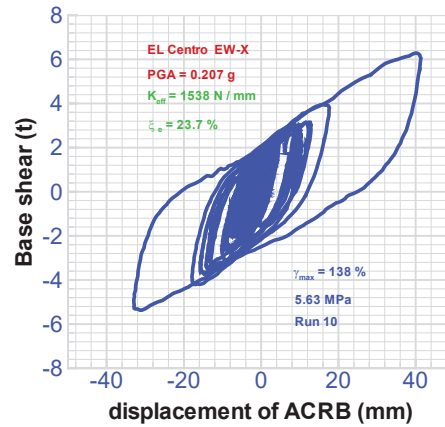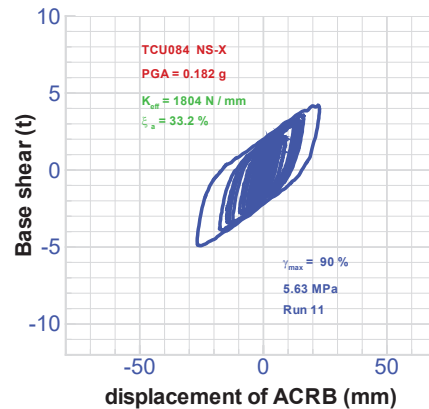Figure 15: Hysteresis loop of ACRB under PGA of 0.182g Chi-Chi NS Earthquake.
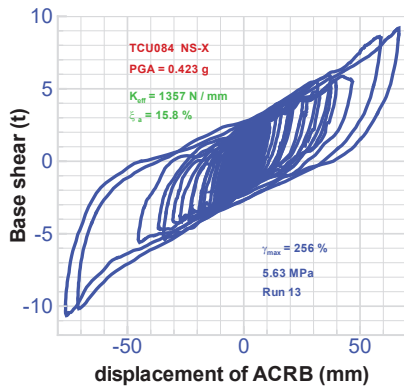
Figure 16: Hysteresis loop of ACRB under PGA of 0.423g Chi-Chi NS Earthquake.

4 CONCLUSIONS

Mass timber buildings are becoming more popular in view of the improved characteristics of laminated timber. Existing bearings such as LRB were already banned due to toxic emission. The performance of its alternative (HDRB) relies on the vertical pressure on the bearing. With the decrease in weight of timber structure compared with conventional concrete or steel structure, it is essential to investigate the possibility of improved bearing which could perform. We manufactured ACRB with carbon fabric. The damping efficiency of ACRB on timber structure was demonstrated under the experiments in this paper. The use of this alternative damper could lower the cost and number of dampers and become more environmental-friendly.

ACKNOWLEDGEMENTS

REFERENCES

[1] Tsai, C. S., Chiang, Tsu-Cheng and Chen, Bo-Jen., 2003, "Component and Shaking Table Tests for Full Scale Multiple Friction Pendulum System", Earthquake Engineering and Structural Dynamics, Vol. 35, No. 13, pp. 1653-1675.

[2] Asher, J. W., Hoskere, S. N., Ewing, R. D., Van Volkinburg, D. R., Mayes, R. L. and Button, M., 1995, "Seismic Performance of the Base Isolated USC University Hospital in the 1994 Northridge Earthquake." Proceedings of the 1995 Joint ASME/JSME Pressure Vessels and Piping Conference, HI, USA, Vol. 319, 147-154.

[3] Dowrick D. J., Babor, J., Cousins, W. J. and Skinner, R. I., 1992, "Seismic Isolation of a Printing Press in Wellington, New Zealand." Bulletin of the New Zealand National Society for Earthquake Engineering, Vol. 25, No. 3, 161-166.

[4] Kalpakidis, I. V. and Constantinou, M. C., 2009a, "Effects of heating on the behaviour of lead–rubber bearings. Ⅰ: theory." Journal of Structural Engineering, ASCE, 135(12):1440-1449 .

[5] Kalpakidis, I. V. and Constantinou, M. C., 2009b, "Effects of heating on the behavior of lead –rubber bearings. Ⅱ:verification of theory." Journal of Structural Engineering, ASCE, 135(12):1450-1461.

[6] Takahashi, Yoshikazu (2012) "Damage of rubber bearings and dampers of bridges in 2011 great East Japan earthquake." Proceedings of the International Symposium on Engineering Lessons Learned from the 2011 Great East Japan Earthquake, March 1-4, 2012, Tokyo, Japan.

[7] Tsai, C. S., 2015 , " Seismic Isolation Devices: History and Recent Developments." In the 2015 ASME Pressure Vessels and Piping Conference, Seismic Engineering, (ed.) by C. S. Tsai, Cleveland, American Society of Mechanical Engineers, Boston, U. S. A.

[8] Mineoh, Takayama, 1997, Road to 4 Seconds Seismic Isolation – Seismic Isolation Structure Design Manual. The Science and Engineering Books.

[9] Tsai, C. S., Chiang, Tsu-Cheng and Chen, Bo-Jen., 2003a, "Component and Shaking Table Tests for Full Scale Multiple Friction Pendulum System", Earthquake Engineering and Structural Dynamics, Vol. 35, No. 13, pp. 1653-1675.

[10] Tsai, C. S., Lu, P. C., Chen, W. S., Chiang, T. C., Yang, C. T. and Lin, Y. C., 2008,"Finite Element Formulation and Shaking Table Tests of Direction-optimized Friction Pendulum System," Engineering Structures, 30(9), 2321-2329).

[11] Ario Cecotti, Carmen Sandhaas, Minoru Okabe, Motoi Yasumura, Chikahiro Minowa and Naohito Kawai, 2013, "SOFIE Project - 3D Shaking Table on a Seven-Storey Full-Scale Cross-Laminated Timber Building", Earthquake Engineering and Structural Dynamics, Vol. 42, pp. 2003-2021.